Magnon-driven longitudinal spin Seebeck effect in $F|N$ and $N|F|N$ structures: role of asymmetric in-plane magnetic anisotropy

L. Chotorlishvili*,[1] Z. Toklikishvili,[2] S. R. Etesami,[1,3] V. K. Dugaev,[1,4,5] J. Barnaś,[6,7] and J. Berakdar[1]

[1] *Institut für Physik, Martin-Luther-Universität Halle-Wittenberg, 06099 Halle, Germany*
[2] *Department of Physics, Tbilisi State University, Chavchavadze av. 3, 0128, Tbilisi, Georgia*
[3] *Max-Planck-Institut für Mikrostrukturphysik, Weinberg 2, 06120 Halle, Germany*
[4] *Department of Physics, Rzeszów University of Technology, al. Powstanców Warszawy 6, 35-959 Rzeszów, Poland*
[5] *Departamento de Física and CFIF, Instituto Superior Técnico, Universidade de Lisboa, Av. Rovisco Pais, 1049-001 Lisbon, Portugal*
[6] *Faculty of Physics, Adam Mickiewicz University, ul. Umultowska 85, 61-614 Poznań, Poland*
[7] *Institute of Molecular Physics, Polish Academy of Sciences, ul. Smoluchowskiego 17, 60-179 Poznań, Poland*

(Dated: September 2, 2015)

The influence of an asymmetric in-plane magnetic anisotropy $K_x \neq K_y$ on the thermally activated spin current is studied theoretically for two different systems; (i) the $F|N$ system consisting of a ferromagnetic insulator (F) in a direct contact with a nonmagnetic metal (N), and (ii) the sandwich structure $N|F|N$ consisting of a ferromagnetic insulating part sandwiched between two nonmagnetic metals. It is shown that when the difference between the temperatures of the two nonmagnetic metals in a $N|F|N$ structure is not large, the spin pumping currents from the magnetic part to the nonmagnetic ones are equal in amplitude and have opposite directions, so only the spin torque current contributes to the total spin current. The spin current flows then from the nonmagnetic metal with the higher temperature to the nonmagnetic metal having a lower temperature. Its amplitude varies linearly with the difference in temperatures. In addition, we have found that if the magnetic anisotropy is in the layer plane, then the spin current increases with the magnon temperature, while in the case of an out-of-plane magnetic anisotropy the spin current decreases when the magnon temperature enhances. Enlarging the difference between the temperatures of the nonmagnetic metals, the linear response becomes important, as confirmed by analytical expressions inferred from the Fokker-Planck approach and by the results obtained upon a full numerical integration of the stochastic Landau-Lifshitz-Gilbert equation.

PACS numbers:

I. INTRODUCTION

One of the key observations that gave impetus to the field of spin caloritronics was the discovery of the spin Seebeck effect (SSE)[1] which amounts to the emergence of a spin current upon an externally applied thermal gradient[2–18]. Technologically, various SSE-based nanoelectronics devices are envisaged. For example, portable thermal diodes have been proposed to control and rectify the heat and spin currents.

The SSE was observed in materials of substantially different transport properties such as metallic ferromagnet Co_2MnSi, semiconducting ferromagnet GaMnAs, and magnetic insulators $LaY_2Fe_5O_{12}$ and (Mn, Ze)Fe_2O_4. Thus, the underlying mechanism may well depend on the specific case under study as well as on the experimental setup. In metallic ferromagnetic systems, the spin is transferred *via* charge carriers activated by the thermal bias, while in magnetic insulators the SSE is mediated by magnons flowing towards the cold edge of the sample. A theory of the magnon driven SSE was developed in Ref. 6 and implemented beyond the linear response regime.[14,15] Thereby, the concept of magnon temperature is of a key importance for understanding the physical origin of the spin current in magnetic insulators: An external heat bias applied to the system thermalizes the phonon subsystem much faster than the magnons relax. Therefore, the magnon temperature T_F^m is influenced by the already established phonon temperature profile T_F. The thermally activated spin current is related to the temperature difference between the phonon and magnon subsystems.

Recent studies based on the macrospin approach (valid for samples of small dimensions on the range of the exchange length) concern the linear[6], and nonlinear response regimes[14]. In both regimes, the obtained analytical expressions for the spin current are proportional to the difference between the phonon and magnon temperatures. As shown in Ref. 14, the result for the spin current obtained in the linear response theory is a particular case of the result obtained in the Fokker-Planck approach, and corresponds to the low magnon temperature regime. The nonlinear effects substantially change the role of the magnetic anisotropy in the formation of the spin current. In the linearized approach, the role of the magnetic anisotropy is similar to that of an external

*levan.chotorlishvili@gmail.com

magnetic field, and can be described by a certain effective field. This is not the case when magnetic fluctuations are large which is more likely for higher temperatures.

A quantitative criterion for the threshold magnon temperature, above which the anisotropy plays an important role, is defined by the following inequality[14], $T_F^m > M_s V H_{\rm eff}/k_B$. Here M_s is the saturation magnetization, V is the total volume of the ferromagnet, and $H_{\rm eff}$ is the effective magnetic field. In the present work we focus on phenomena inherent to the nonlinear regime. In particular, we study the influence of the in-plane magnetic anisotropy on the SSE. We show that the effect of the in-plane anisotropy on the thermally activated spin current is different from the effect of the uniaxial out-of-plane anisotropy studied in Ref. 14.

We consider two different system relevant for the longitudinal SSE: (i) an $F|N$ structure consisting of a ferromagnetic insulating part (F) attached to a nonmagnetic metallic part (N), and (ii) a ferromagnetic insulating part sandwiched between two nonmagnetic metallic ones ($N|F|N$). In the following the nonmagnetic metallic part will be referred to as metallic part or simply as metal, while the ferromagnetic insulating part will be referred to as ferromagnetic part or simply as ferromagnet. We show that in the both cases thermally activated spin current is parallel to the temperature gradient. In the case of $N|F|N$ structure we show that if the difference between the temperatures of the two metals is not large, and the temperature dependance of the spin conductance can be ignored, then the spin pumping currents from the ferromagnet to the adjacent metals are equal in amplitude and are oriented oppositely, so they do not contribute to the total spin current. The only contribution to the total spin current is then due to the spin torque current. We show that the spin torque current flowing through the ferromagnetic part is a linear function of the difference between the temperatures of the two metals. Though, the considerations apply directly to the case when the ferromagnetic part is insulating, the results are also applicable when the ferromagnetic part is metallic.

In Section 2 we present the model F/N structure. The Fokker-Planck approach is briefly described in Section 3, where analytical results for the spin current in the $F|N$ system are presented. Numerical results for the total spin current in the $F|N$ system, obtained by a direct numerical integration of the stochastic Landau-Lifshitz-Gilbert (LLG) equation, are presented and discussed in Section 4. We show that in the presence of an in-plane magnetic anisotropy and a weak magnetic field, the ($F|N$) system supports a spin pumping current only if the axial symmetry in the system is broken by an in-plane magnetic anisotropy. In Section 5 we discuss analytical results on the spin current flowing through the system $N|F|N$, while the corresponding results obtained by numerical integration are presented in Section 6. We show that such a system supports spin pumping current only for a sufficiently large thermal gradient. Summary and final conclusions are in Section 7.

II. MODEL OF THE $F|N$ STRUCTURE

We consider first the thermally activated spin current through the interface in the $F|N$ system. Our main focus is on the influence of the in-plane magnetic anisotropy, $-M_s\big(K_x m_x^2 + K_y m_y^2\big)/2$, on the spin current. Here, $\mathbf{m}$ is a unit vector along the magnetic moment, $\vec{m} = \vec{M}/M_s$. We assume that the thermal equilibrium between the electron and the phonon subsystems in the metallic part as well as in the ferromagnetic part is restored internally much faster than the equilibrium between the two parts. In terms of the local temperature, which is based on the hierarchy of relaxation times, this means that the temperatures of the phonons, $T^p_{N(F)}$, and the electrons $T^e_{N(F)}$, baths are equal in both the metallic and ferromagnetic parts, $T^p_N = T^e_N = T_N$, $T^p_F = T^e_F = T_F$. However, there is a difference in temperatures of the two components, $T_F \neq T_N$, which can be controlled externally. This difference drives the SSE. The interaction between the nonmagnetic and ferromagnetic subsystems is mediated *via* the magnon bath, described by the magnon temperature T_F^m. Due to the slower magnon relaxation, T_F^m may be different from T_F.

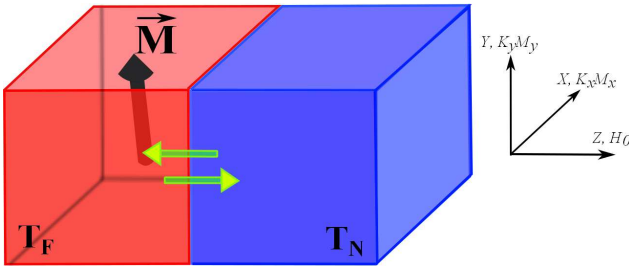

FIG. 1: A schematic illustration of the considered $F|N$ system. The system consists of a ferromagnetic insulator (left) and a nonmagnetic metal (right) in direct contact. The temperatures of the ferromagnetic (T_F) and metallic (T_N) parts are in general different.

The magnetization dynamics of the ferromagnetic part, to be considered in the following section, is described by the LLG equation in the macrospin approximation. Such an approach excludes nonuniform magnetization, and therefore is applicable when the magnetic component of the system has a small volume, i.e., its lateral and vertical dimensions are small, usually in the nanometer range. Using the Fokker-Plank-equation technique, we evaluate the mean value of the spin current flowing through the interface from the ferromagnetic part to the metallic one. We also study there the dependence of the total spin current on the in-plane magnetic anisotropy.

III. FOKKER-PLANCK APPROACH: ANALYTICAL SOLUTION FOR THE SPIN CURRENT IN THE $F|N$ SYSTEM

The total spin current flowing through the interface in the $F|N$ system consists of two contributions – the spin pumping current flowing from the ferromagnet to the normal metal, and the thermally activated spin current flowing in the opposite direction (in the following also referred to as the spin torque current). Powered by the phonon bath, thermal noise leads to formation of the fluctuating spin torque current in the normal metal, $\vec{I}_{fl}(t)$. Effect of this fluctuating spin torque current on the ferromagnetic insulator can be described by a random magnetic field $\vec{h}'(t)$ acting on the magnetization,[6] $\vec{I}_{fl}(t) = -\frac{M_sV}{\gamma}\gamma\vec{m}(t)\times\vec{h}'(t)$. Here M_s is the saturation magnetization, V is the total volume of the ferromagnet, and γ is the gyro-magnetic factor. On the other hand, the thermally activated magnetization dynamics in the ferromagnet gives rise to a spin pumping current emitted from the ferromagnet into the normal metal, $\vec{I}_s = \frac{M_sV}{\gamma}\alpha'\vec{m}\times\dot{\vec{m}}$. Thus, the total average *dc* spin current across the interface can be written in the form[6,14]

$$\langle\vec{I}_s\rangle = \frac{M_sV}{\gamma}\left[\alpha'\langle\vec{m}\times\dot{\vec{m}}\rangle - \gamma\langle\vec{m}\times\vec{h}'\rangle\right], \tag{1}$$

where , $\alpha' = (\gamma\hbar/4\pi M_sV)g_r$ is the magnetization damping constant (related to the spin pumping), and g_r is the real part of the dimensionless spin mixing conductance. Furthermore, $\vec{h}'(t)$ is the random magnetic field. If the random thermal force has correlation time much shorter than the response time of the system, one can assume that the noise is white. A quantitative criterion for using a white noise is[6] $k_BT \gg \hbar\omega_0$, where ω_0 is the ferromagnetic resonance frequency. Taking into account the fact that the response time of the system is defined by $\omega_0 \approx 1$ GHz, for the low temperature limit one obtains $T >> 0.01$K. Evidently, this temperature regime allows using the white noise in our problem[19,20]:

$$\langle\gamma h_i'(t)\ \gamma h_j'(t')\rangle = \sigma'^2\delta_{ij}\delta(t-t'), \tag{2}$$

for $i,j = x,y,z$, where $\sigma'^2 = 2\alpha'\gamma k_BT_N/M_sV$. Thus, to find the spin current we need to know the time evolution of the magnetization. The magnetization dynamics is described by the stochastic LLG equation for the dimensionless unit vector $\vec{m}$

$$\dot{\vec{m}} = -\gamma\vec{m}\times\left(\vec{H}_{\rm eff}+\vec{h}\right) + \alpha\vec{m}\times\dot{\vec{m}}. \tag{3}$$

The effective magnetic field $\vec{H}_{\rm eff}$ consists of the external field applied along the z axis and of the in-plane magnetic anisotropy field $\vec{h}_A = -\partial V_{\rm an}/\partial\vec{M} = K_xm_x\vec{i}_x + K_ym_y\vec{i}_y$, where $\vec{i}_{x(y)}$ are the unit vectors along the axis $x(y)$. The magnetic anisotropy energy density, $V_{\rm an} = -\frac{1}{2}M_s(K_xm_x^2 + K_ym_y^2)$, is described by the anisotropy constants K_x and K_y. In the above equation, α is the total magnetic damping constant, $\alpha T_F^m = \alpha_0T_F + \alpha'T_N$. This damping constant includes the contributions from the standard bulk damping constant α_0 which is associated with the lattice thermal oscillations (Gilbert damping) and from the damping constant α' associated with the contact to the normal metal. Introducing the enhanced total damping constant α has a clear physical motivation. Due to the effect of the $F|N$ interface, magnetization dynamics in the F layer is additionally damped, and this enhanced damping is due to a magnonic spin current transferred from the ferromagnetic insulator to the normal metal.[21] Also here we assumed that the random contributions from the uncorrelated noise sources are totally independent and, therefore, the total enhanced damping constant is factorized[6]. Finally, $\vec{h}$ in Eq.(3) is the total random field, with the corresponding correlation function of the form[6]

$$\langle h_i(t)h_j(t')\rangle = \sigma^2\delta_{ij}\delta(t-t'), \tag{4}$$

where $\sigma^2 = 2\alpha k_BT_F^m/M_sV\gamma$ is the coefficient proportional to the magnon temperature.

Following the procedure described in Ref. 14, we derive the Fokker-Planck (FP) equation for the distribution function $f(\vec{m},T)$:

$$\frac{\partial f}{\partial t} = \frac{1}{1+\alpha^2}\frac{\partial}{\partial\vec{m}}\Bigg\{(\vec{m}\times\vec{\omega}_{\rm eff})\,f + \alpha\vec{m}\times(\vec{m}\times\vec{\omega}_{\rm eff})\,f - \frac{\sigma^2}{2(1+\alpha^2)}\vec{m}\times\left(\vec{m}\times\frac{\partial f}{\partial\vec{m}}\right)\Bigg\}, \tag{5}$$

where $\vec{\omega}_{\rm eff} = \gamma\vec{H}_{\rm eff} = (\omega_xm_x, \omega_ym_y, \omega_0)$. The stationary solution of the FP equation reads:

$$f(\vec{m}) = Z^{-1}\exp\left(\beta\int\vec{\omega}_{\rm eff}.d\vec{m}\right), \tag{6}$$

where $Z = \int\exp\left(\beta\int\vec{\omega}_{\rm eff}\cdot d\vec{m}\right)d^3\vec{m}$ is the normalization factor, and we introduced the following notation: $\beta = 2\alpha\left(1+\alpha^2\right)/\sigma^2$. Taking into account Eqs. (1) to (6), after some cumbersome, but straightforward calculations we find the following expression for the average total spin current:

$$\langle I_{sz}\rangle = \alpha' k_B\Big\{T_F^mA\langle1-m_z^2\rangle - 2T_F^mB_x\langle m_zm_x^2\rangle - 2T_F^mB_y\langle m_zm_y^2\rangle - 2T_N\langle m_z\rangle\Big\}, \tag{7}$$

where $A = \frac{M_sVH_0}{k_BT_F^m}$, $B_x = \frac{K_xM_sV}{2k_BT_F^m}$, and $B_y = \frac{K_yM_sV}{2k_BT_F^m}$, while the averages occurring in Eq. (7) are defined in the Appendix [see Eqs. (A1) to (A5)]. By definition, the spin current is generally a second rank tensor and is characterized by spatial orientation and projection of momentum, $I_{x,y,z}^{M_{x,y,z}}$. However, due to the particular geometry under consideration, only the longitudinal spin current

component, $I_z^{M_z} = I_{sz}$, is nonzero, while the transversal spin current components vanish, $I_{sx} = I_{sy} = 0$. Thus our findings are in favor of the recent experiment[22] in which upper limit for the transverse spin Seebeck effect was observed several orders of magnitude smaller than previously reported. In spite of the fact that expression of the spin current doesn't depend on the enhanced damping constant α explicitly, due to the relation $\alpha T_F^m = \alpha_0 T_F + \alpha' T_N$ spin current still depends on α implicitly. One can invert dependence on the spin mixing conductance damping α' into the dependence on α. However precise values of α' is too much related to the characteristics of particular interface. Therefore for the sake of general interest we quantify spin current in terms of $< I_{sz} > /\alpha' k_B$. The in-plane magnetic anisotropy has different physical consequences, when compared to the case of an out-of-plane anisotropy studied in Ref. 14. First of all, the expression for the total spin current in the case of an in-plane anisotropy is different from that for an out-of-plane anisotropy. Only in the case of an axial symmetry, $K_x = K_y$, the expressions for the total spin current become partly similar. However, as we will see below, the main effect of the in-plain anisotropy concerns the asymmetric case, $K_x \neq K_y$.

The expression for the total spin current, Eq. (7), is quite general. Therefore, we consider now some asymptotic situations. In the symmetric case, $K_x = K_y = H_A$, one finds $B_x = B_y = B = H_A M_s V/2k_B T_F^m$. Equation (7) reduces then to a simpler form, while the mean components of the magnetization can be calculated analytically:

$$\langle m_z \rangle = \frac{A}{2B} + \frac{2}{\sqrt{\pi B}} \frac{e^{-\frac{A^2}{4B}-B} \sinh[A]}{G(A,B)}, \tag{8a}$$

$$\langle 1 - m_z^2 \rangle = 1 - \left(\frac{A}{2B}\right)^2 - \frac{1}{2B} - \frac{e^{-\frac{A^2}{4B}-B}(2B\cosh(A) + A\sinh(A))}{G(A,B)}, \tag{8b}$$

$$\langle m_z \left(m_x^2 + m_y^2\right) \rangle = -\left(\frac{A}{2B}\right)^3 - \frac{3}{4}\frac{A}{B^2} + \frac{A}{2B} - \frac{e^{-\frac{A^2}{4B}-B}}{2\sqrt{\pi}B^{5/2}G(A,B)} \times \left[2AB\cosh(A) + \left(A^2 + 4B\right)\sinh(A)\right]. \tag{8c}$$

Here, we introduced the following notation: $G(A,B) = \mathrm{erf}\left((A-2B)/2\sqrt{B}\right) - \mathrm{erf}\left((A+2B)/2\sqrt{B}\right)$, where $\mathrm{erf}(\cdots)$ is the error function. Interestingly, the in-plane magnetic anisotropy in the symmetric case is equivalent to the out-of-plane anisotropy, $-H_A m_z^2$. Therefore, after substituting $B \to -B$ in Eqs (8), we recover the results derived earlier[14].

In the case of weak magnetic anisotropy, $B < 1$, the mean components of the magnetic moment can be further simplified (see Eq. (A6) to Eq. (A9) in the Appendix). In turn, in the absence of magnetic anisotropy, $B \to 0$, from Eqs. (7) and (8) one finds $\langle m_z \rangle = L(A)$, $\langle (1 - m_z^2) \rangle = 2L(A)/A$, and $\langle I_{sz} \rangle = 2\alpha' k_B L(A)(T_F^m - T_N)$, where $L(A) = \coth(A) - 1/A$ is the Langevin function. This result (obtained for $B \to 0$) recovers the previously obtained expression for the total spin current[14].

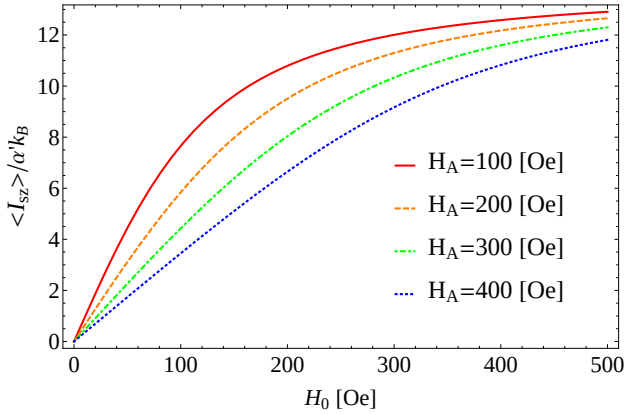

FIG. 2: Dependence of the average total spin current $\langle I_{sz} \rangle/\alpha' k_B$ on the external magnetic field H_0 for the following parameters: $K_x = K_y = H_A > 0$ (with H_A as indicated), $T_F^m = 300$ K, $T_N = 297$ K, $M_s = 800$ G, and $V = 1.6 \times 10^{-18}$ cm^3. The figure shows that the spin current decreases with the increasing the magnetic anisotropy. Since we measure spin current in the units of $\langle I_{sz} \rangle/\alpha' k_B$ spin current doesn't depend on the α'. Besides analytical result is obtained via the steady sate solution of the FP equation. This implicates that system is already relaxed. This is reason why spin current doesn't depend on the α as well. Values of the inverse damping constant $1/\alpha$ defines relaxation rate and steady sate distribution function is formed beyond this time scale.

Now we address the case of a high magnon temperature, $M_s V H_0/k_B T_F^m < 1$ and $H_A M_s V/2k_B T_F^m < 1$. Then, from Eqs. (7) and (8) we obtain $\langle I_{sz} \rangle = 2\alpha' k_B \frac{M_s V H_0}{3k_B T_F^m} (T_F^m - T_N) \left(1 - \frac{2}{3}\frac{H_A M_s V}{2k_B T_F^m}\right)$ for the total spin current. From this formula follows that the positive in-plane anisotropy ($H_A > 0$) reduces the total spin current, while the negative in-plane anisotropy ($H_A < 0$) enhances the total spin current. Apart from this, the spin current is proportional to the difference $(T_F^m - T_N)$ between the magnon temperature and the temperature of the metal. The amplitude of the total spin current, however, is reduced because of the anisotropy term $\frac{2}{3}\frac{H_A M_s V}{2k_B T_F^m}$. Another interesting observation is that the spin current vanishes, $\langle I_{sz} \rangle \to 0$, for zero magnetic field, $H_0 \to 0$. This result is rather clear since the dynamics of the magnetization is then strongly exposed to the thermal fluctuations, and therefore suppresses the spin current generation.

In the case of a strong magnetic field and a weak anisotropy, $\frac{1}{2}H_A M_s V < k_B T_F^m < H_0 M_s V$, we enter a different regime, and the expression for the total spin

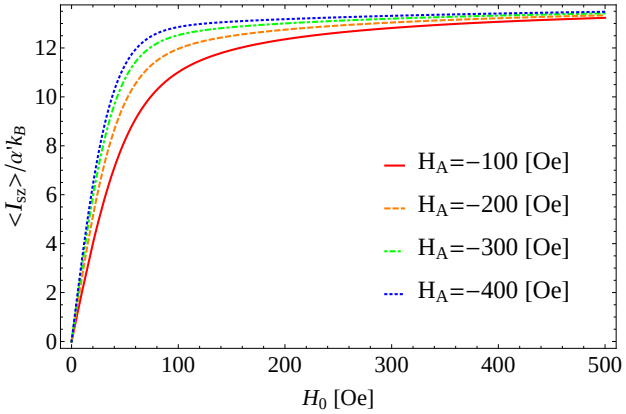

FIG. 3: The average total spin current as function of the external magnetic field H_0 for the following parameters: $K_x = K_y = H_A < 0$ (with H_A as indicated), $T_F^m = 300$ K, $T_N = 297$ K, $M_s = 800$ G, and $V = 1.6 \times 10^{-18}$ cm^3. Absolute values of the magnetic anisotropy field are the same as in Fig. 2, but here they have the opposite sign. Note, the spin current now increases with increasing $|H_A|$.

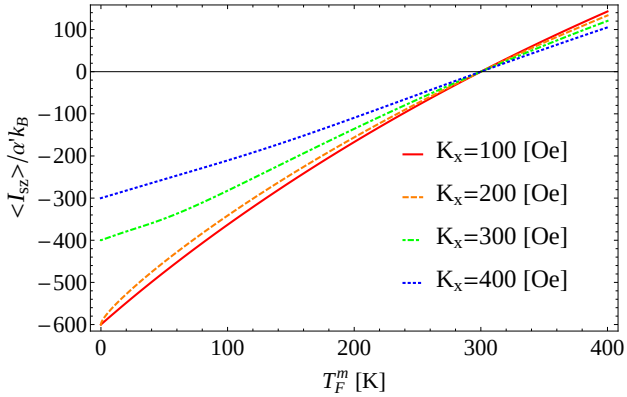

FIG. 4: The average total spin current as the magnon temperature T_F^m varies. The following parameters are chosen: $K_y = 100$ Oe, $H_0 = 200$ Oe, $T_N = 300$ K, $M_s = 800$ G, $V = 1.6 \times 10^{-18}$ cm^3, and K_x as indicated.

current in this regime reads

$$\langle I_{sz} \rangle = 2\alpha' k_B \left(T_F^m - T_N\right)\left(1 - \frac{3H_A}{H_0}\frac{k_B T_F^m}{M_s V H_0}\right). \qquad (9)$$

The first term in Eq. (9) is the standard contribution to the spin current in the linear response, while the second term is due to the magnetic anisotropy. As before, the positive in-plane anisotropy ($H_A > 0$) suppresses the total spin current, while the negative in-plane anisotropy ($H_A < 0$) enhances the spin current.

Having considered some limiting asymptotics for the thermally activated spin current, let us go back to the general solution, see Eqs. (7) and (8). Since the general solution is relatively complex for its illustration we plot the total average spin current as a function of the external magnetic field H_0 and the magnon temperature T_F^m. First, we consider a symmetric situation, $K_x = K_y = H_A$, and then proceed with more important an asymmetric case, $K_x \neq K_y$.

Figures 2 and 3 show the dependence of the total spin current on the external magnetic field H_0 applied along the z axis. As one can note, the magnitude of spin current depends on the sign of the anisotropy field H_A. For positive magnetic anisotropy, Fig. 2, the spin current decreases with increasing the anisotropy field, while for negative anisotropy, the spin current grows with increasing absolute value of H_A, see Fig. 3. In turn, the dependence of the average spin current on the magnon temperature is presented in Fig.4 for the indicated values of the anisotropy constant K_x and the constant K_y. All curves cross at the point $T_F^m = T_N$, where the spin current is equal to zero as the system is then in thermal equilibrium. Interestingly, the spin current for $K_x > K_y$ is reduced in comparison to the spin current in the symmetrical case ($K_x = K_y$). This is because the x-component of magnetization increases with the increasing constant K_x (positive), and thus the magnetization projection on the z-axis becomes reduced.

Before proceeding to a more important case of asymmetric in-plane anisotropy ($K_x \neq K_y$), we plot the dependence of the mean magnetization component $\langle m_z \rangle$ on the applied magnetic field. As follows from Fig. 5, the magnetization component $\langle m_z \rangle$ increases with the applied magnetic field, approaching the maximum $\langle m_z \rangle \approx 1$. However, the limit $\langle m_z \rangle = 1$ corresponds to the zero magnon temperature, $A = \frac{M_s V H_0}{k_B T_F^m} \to \infty$, $T_F^m = 0$, and therefore is beyond the Fokker-Plank approach.

Finally, let us consider the limit of low magnon temperature. Taking into account Eq. (6), Eq. (7), and applying the saddle-point method, we find the following formula for the average total spin current in the limit of a weak magnetic field $2H_0/(K_x + K_y) < 1$:

$$\langle I_{sz} \rangle = -\alpha' k_B \eta_1 \left\{ \eta_2 \frac{I_1(\eta_2/T_F^m)}{I_0(\eta_2/T_F^m)} + T_N \right\}. \qquad (10)$$

Here, we introduced the following notation: $\eta_1 = H_0/(K_x + K_y)$ and $\eta_2 = \frac{M_s V}{4k_B}(K_x - K_y)\left(1 - 4\eta_1^2\right)$. In the opposite case of $2H_0/(K_x + K_y) > 1$, the spin current is given by the expression $\langle I_{sz} \rangle = -2\alpha' k_B T_N$.

The second term in Eq. (10) corresponds to the spin torque current flowing from the metal to the ferromagnet, so it is negative, $-\alpha' k_B \eta_1 T_N$. Taking into account the parity of Bessel functions $I_1(\eta_2/T_F^m)$ and $I_0(\eta_2/T_F^m)$, it is easy to see that the first term $-\alpha' k_B \eta_1 \eta_2 I_1(\eta_2/T_F^m)/I_0(\eta_2/T_F^m)$ is even with respect to

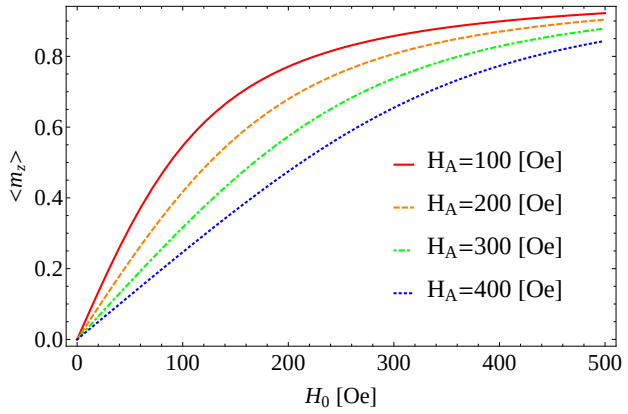

FIG. 5: Dependence of the averaged component of magnetization $\langle m_z \rangle$ on the external magnetic field H_0 for the following parameters: $K_x = K_y = H_A > 0$ (with H_A as indicated), $T_F^m = 300$ K, $T_N = 297$ K, $M_s = 800$ G, and $V = 1.6 \times 10^{-18}$ cm^3. The magnetic field $H_0 = (0, 0, H_0)$ tends to align magnetization vector along the Z axis, while the in-plane magnetic anisotropy favors the in-plane alignment of the magnetization.

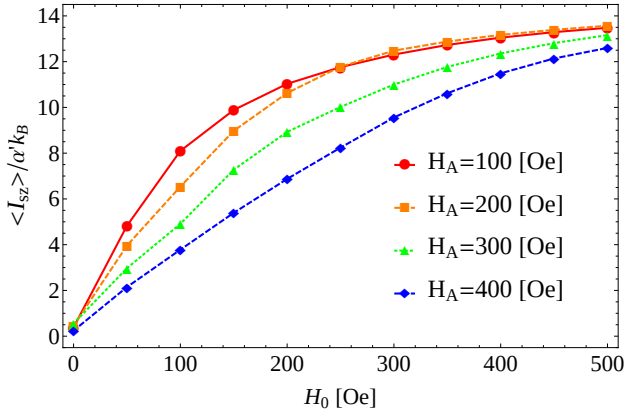

FIG. 6: The total spin current as a function of the external magnetic field H_0, obtained *via* numerical integration of the stochastic LLG equation for the indicated values of the positive anisotropy constant H_A and for the parameters: $T_F^m = 300$ K, $T_N = 297$ K, $M_s = 800$ G, $V = 1.6 \times 10^{-18}$ cm^3, $\alpha = 1.0$ and $\alpha' = 0.05$.

the permutation $(K_x - K_y) \to -(K_x - K_y)$, and is always negative. It disappears in the symmetric case of $K_x = K_y$ while in the antisymmetric case it decreases the spin torque current, see Fig. 4 in the low magnon temperature regime.

IV. NUMERICAL SOLUTIONS FOR THE $F|N$ SYSTEM

The results derived analytically in the previous section from the solution of the Fokker-Planck equation can be further confirmed by exact numerical integration of the stochastic LLG equation, assuming the random field $\vec{h}$ as a Gaussian white noise defined through the correlation function, see Eq. (4). The magnon temperature T_F^m is implemented into the simulations *via* the strength parameter of the correlation function, $\sigma^2 = 2\alpha k_B T_F^m / M_s V \gamma$ (see also section 3).

To solve the stochastic LLG equation we used the Heun method, which converges in the quadratic mean to the solution interpreted in the sense of Stratonovich[23]. From the solutions of the stochastic LLG equation we generated the random trajectories for a sufficiently long time interval, until the magnetization components reached the stationary regime. This procedure has been implemented many times in order to construct an ensemble of the random solutions of the stochastic LLG equation[24]. Each of these random solutions corresponds to a certain realization of the random noise, while the statistical average over the ensemble of realizations designates the mean values of the magnetization components. Such average components of the magnetization vector ($\vec{m}$ and $\dot{\vec{m}}$) can be used afterwards for the evaluation of spin current. This numerical procedure is in general computationally expensive[25], since the number of realizations needed to reach a good accuracy of the solution to the stochastic LLG equation is about one thousand.[15].

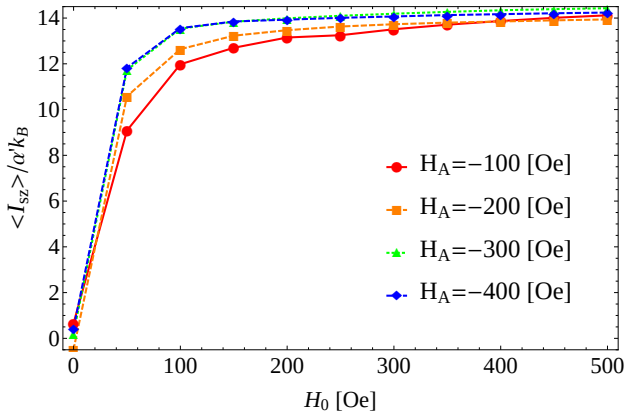

FIG. 7: Total spin current as a function of an external magnetic field H_0, obtained *via* a numerical integration of the stochastic LLG equation for the indicated values of the negative anisotropy constant, and for the parameters: $T_F^m = 300$ K, $T_N = 297$ K, $M_s = 800$ G, $V = 1.6 \times 10^{-18}$ cm^3, $\alpha = 1.0$ and $\alpha' = 0.05$.

This numerical procedure can be used to calculate the spin pumping current from the ferromagnetic part to the metallic one (first term in Eq. (1)). In order to calculate the spin torque current from the metal to the ferromagnet (second term in Eq. (1)), we have to consider the random magnetic field in the metallic part, $\vec{h}'$, and the corresponding correlation function, Eqs. (2). The metal

temperature T_N is interlaced with the strength of this stochastic field, $2\alpha' k_B T_N/M_s V\gamma$.

Results of the numerical simulations are presented in Figs. 6 and 7. As we see, the numerical results for the total spin current are very close to the results obtained by means of the Fokker-Planck equation, see Fig. 2 and Fig. 3. In both cases, the total spin current increases with an external magnetic field. In the case of a positive anisotropy field, the larger is the anisotropy, the smaller is the spin current, while in the case of a negative anisotropy field, the spin current increases with increasing the anisotropy field.

V. SPIN CURRENT IN $N|F|N$ STRUCTURES

The technique used above can be also employed to calculate the thermally-induced spin current in a $N|F|N$ system, shown schematically in Fig. 8. Now, the total spin current includes four terms,

$$\vec{I}_s = \vec{I}_{fl1} + \vec{I}_{sp1} + \vec{I}_{fl2} + \vec{I}_{sp2}, \tag{11}$$

where $\vec{I}_{sp1}$ and $\vec{I}_{sp2}$ stand for the spin pumping current from the ferromagnet to the metallic parts $N1$ (left) and $N2$ (right), respectively (see Fig. 8). In turn, $\vec{I}_{fl1}$ and $\vec{I}_{fl2}$ stand for the spin torque current flowing, respectively, from the left and right metallic parts to the ferromagnetic one due to thermal fluctuations. We assume that the two metals have generally different temperatures, T_{N1} and T_{N2}.

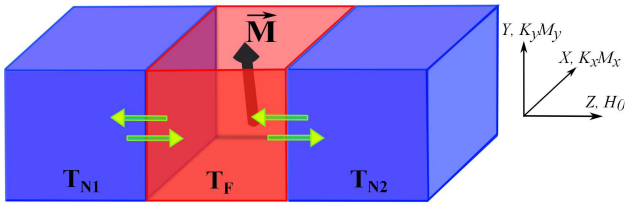

FIG. 8: Schematic presentation of the $N|F|N$ structure consisting of a magnetic element sandwiched between two nonmagnetic parts – $N1$ on the left and $N2$ on the right side. Temperatures of the parts $N1$ and $N2$ are generally different.

Upon laborious calculations, one finds the components of the spin pumping current flowing from the ferromagnet towards the two ($i = 1, 2$) metallic parts,

$$\begin{aligned}\langle I_{sp}^{(1)}\rangle &= -\frac{M_s V}{\gamma}\alpha'\big(T_{N1}\big) f\big(T_F^m\big),\\ \langle I_{sp}^{(2)}\rangle &= \frac{M_s V}{\gamma}\alpha'\big(T_{N2}\big) f\big(T_F^m\big),\end{aligned} \tag{12}$$

where, for shortness, we introduced the following function:

$$\begin{aligned}f\big(T_F^m\big) &= \langle\omega_z^{\rm eff}\big(1-m_z^2\big)\rangle\\ &- \langle\omega_x^{\rm eff} m_z m_z\rangle - \langle\omega_y^{\rm eff} m_z m_y\rangle.\end{aligned} \tag{13}$$

In turn, for the spin torque components we find

$$\begin{aligned}\langle I_{fl}^{(1)}\rangle &= 2k_B\langle m_z\rangle\alpha'\big(T_{N1}\big)T_{N1},\\ \langle I_{fl}^{(2)}\rangle &= -2k_B\langle m_z\rangle\alpha'\big(T_{N2}\big)T_{N2}.\end{aligned} \tag{14}$$

As one can see from Eqs. (13) and (14), the difference in the two components of the spin pumping current transferred from the ferromagnetic part to the metals, $\langle I_{sz}^{(1)}\rangle$ and $\langle I_{sz}^{(2)}\rangle$, is related to the temperature dependence of the damping constants, or, more precisely, to the temperature dependence of the spin conductance, $\alpha'\big(T_N\big) = \frac{\gamma\hbar}{4\pi M_s V} g_r\big(T_N\big)$. Such a temperature dependence of the spin conductance $g_r\big(T_N\big)$ has been measured in a recent experiment[26].

For convenience, we denote $\alpha'\big(T_{N1}\big) = \alpha'$ and $\alpha'\big(T_{N2}\big) = \alpha' + \Delta\alpha'$, and rewrite the expression for the total spin current in the form

$$\begin{aligned}\langle I_{sz}\rangle &= 2k_B\langle m_z\big(T_F^m\big)\rangle\alpha'\big(T_{N1}-T_{N2}\big)\\ &+ \frac{M_s V}{\gamma} f\big(T_F^m\big)\triangle\alpha' - 2k_B\langle m_z\big(T_F^m\big)\rangle\Delta\alpha' T_{N2}.\end{aligned} \tag{15}$$

If the difference between the temperatures of the metals, T_{N1} and T_{N2}, is not too large, then the variation of the damping constant $\Delta\alpha'$ is very small, $\Delta\alpha' \ll \alpha'$. In particular, the experimental data show the following change of the damping constant with temperature:[26] if $\Delta T = T_{N1} - T_{N2} \approx 350$K then $|\Delta\alpha'|/\alpha' \approx 0.28$. For $T_{N1} - T_{N2} < 100$ the relative variation of the damping constant is even smaller, $|\Delta\alpha'|/\alpha' < 0.1$. In such a case, the spin pumping currents transferred into the metals almost compensate each other, $\vec{I}_{sp1} \approx -\vec{I}_{sp2}$. Thus, if the difference between the temperatures of the metals, T_{N1} and T_{N2}, is not high, the $N|F|N$ system becomes nearly symmetric, and only the spin torque current contributes to the total spin current. The ferromagnetic part serves then as a conductor which transfers the spin current from the hot metal to the cold one. We note, that though the spin pumping currents to the left and right metals do not contribute to the total current, $\vec{I}_{sp1} \approx -\vec{I}_{sp2}$, they lead to an enhanced Gilbert damping α' in Eq. (15).

Hence, in the symmetric case, the calculation of the total spin current is greatly simplified, and the expression for the total spin current reads

$$\langle I_{sz}\rangle = 2\alpha' k_B\langle m_z\rangle\big(T_{N1}-T_{N2}\big). \tag{16}$$

As follows from Eq. (16), the spin current flowing through the ferromagnet mostly depends on the temperature difference between the metals. However, an additional temperature dependence enters through the mean value of the magnetization $\langle m_z\rangle$, which is a function of the magnon temperature T_F^m.

In the absence of magnetic anisotropy and in the limit of a weak external magnetic field, $M_s V H_0 << k_B T_F^m$, the expression for the spin current takes the form

$$\langle I_{sz}\rangle = \frac{2}{3}\alpha' M_s V H_0 \frac{T_{N1}-T_{N2}}{T_F^m}. \tag{17}$$

Obviously, the spin current decreases upon enhancing the magnon temperature. From the physical point of view this result is rather clear. The magnetic part conducts the spin torque current from the hot normal metal to the cold one, and the resistance of magnetic element is increasing with the magnon temperature T_F^m. Therefore, the spin current decreases at the elevated magnon temperature.

In the limit of a weak external magnetic field, $M_s V H_0 << k_B T_F^m$, the out-of-plane magnetic anisotropy leads to the following correction in the spin current formula,

$$\langle I_{sz}\rangle = \frac{2}{3}\alpha' M_s V H_0 \frac{T_{N1}-T_{N2}}{T_F^m}\left(1+\frac{2M_s V H_A}{15 k_B T_F^m}\right). \quad (18)$$

Thus, in the case of out-of-plane magnetic anisotropy, the spin current always decreases with increasing the magnon temperature T_F^m. This result is clear since the magnetic anisotropy tends to align the magnetic moment along the z axis, and thus increases the spin current in accordance with Eq. (16), while the high magnon temperature T_F^m reduces $\langle m_z\rangle$ and thus decreases the spin current.

In the case of in-plane magnetic anisotropy, the expression for the current reads

$$\langle I_{sz}\rangle = \frac{2}{3}\alpha' M_s V H_0 \frac{T_{N1}-T_{N2}}{T_F^m}\left(1-\frac{2M_s V H_A}{15 k_B T_F^m}\right). \quad (19)$$

Thus, the temperature dependence is similar in both cases. The difference concerns the role of magnetic anisotropy – the out-of-plane anisotropy increases the spin current whereas the in-plane magnetic anisotropy reduces the spin current.

VI. NUMERICAL RESULTS FOR THE $N|F|N$ STRUCTURE

As in the case of the $F|N$ structure, the analytical results derived above for the $N|F|N$ system can be supported by direct numerical integration of the stochastic LLG equation for the corresponding macrospin. Instead of this, we go in this section beyond the macrospin approximation. It is well known, that the macrospin description breaks down for non-uniformly magnetized samples with the characteristic lengths exceeding several tens of nm's. Beyond the macrospin formulation, the SSE effect can be described by introducing the local magnetization $\vec{m}(\vec{r},t)$. The description can be then reduced to a discrete chain of magnetic moments.

As shown in recent work of Etesami et al.[15], the spin current in the case of discrete chain of magnetic moments can be calculated by using the following recurrent relations

$$I_n = 2Aa\sum_{l=1}^{n} m_l^{\mathrm{x}}(m_{l-1}^{\mathrm{y}}+m_{l+1}^{\mathrm{y}}) - m_l^{\mathrm{y}}(m_{l-1}^{\mathrm{x}}+m_{l+1}^{\mathrm{x}}), \quad (20)$$

where A is the exchange stiffness, a is the unit cell size, m_i^x, m_i^x are the components of the individual magnetic moments, and I_n is the site-dependent spin current. We note that in the case of a non-uniformly magnetized sample, the spin current is not uniform along the chain. The chain is oriented along the x axes and the easy axes is in the z direction.

The dynamics of magnetic moments $\vec{m}_n$ is described by coupled stochastic LLG equations, we have to solve numerically. For more technical details we refer to the recent work of Etesami et al.[15]. The way how we take into consideration the interface effects is straightforward. Namely, the contact of the magnetic chain with the left and right metallic parts leads to modification of the damping constant for the first and last magnetic moments, $\alpha_{1,N} = \alpha + \gamma\hbar g_{\mathrm{eff}}/(4\pi a M_s)$, where g_{eff} is the effective spin-mixing constant at the interfaces. Constant $\alpha_{1,N}$ models enhancing of the Gilbert damping and is related to the spin pumping current. For more details see[21]. The other point is that in the equations of motion for the first and last magnetic moments, which are in contact with the left and right normal metals, include the spin torque term.

The idea of the spin torque is that it accounts for the effect of the interface on the adjacent magnetic moments[15,25]. We assume that the ratio between the amplitudes of the spin torque terms is proportional to the ratio of the temperatures of the two metals, $|\vec{I}_{\mathrm{L}}^{\mathrm{in}}|/|\vec{I}_{\mathrm{R}}^{\mathrm{in}}| = T_L^N/T_R^N$ and $\vec{I}_{\mathrm{L}}^{\mathrm{in}} = \lambda(T_L^N,0,0)$ and $\vec{I}_{\mathrm{R}}^{\mathrm{in}} = \lambda(-T_L^R,0,0)$, where λ is a phenomenological constant.

Thus, the equation of motion for the magnetic moment $\vec{m_n}$ can be written as

$$\begin{aligned}\frac{\partial \vec{m}_n}{\partial t} = &-\frac{\gamma}{1+\alpha_n^2}\left[\vec{m}_n\times\vec{H}_n^{\mathrm{eff}}\right]\\ &-\frac{\gamma\alpha_n}{(1+\alpha_n^2)}\left[\vec{m}_n\times\left[\vec{m}_n\times\vec{H}_n^{\mathrm{eff}}\right]\right],\end{aligned} \quad (21)$$

for $n = 2,...N-1$, and

$$\begin{aligned}\frac{\partial \vec{m}_{1,N}}{\partial t} = &-\frac{\gamma}{1+\alpha_{1,N}^2}\left[\vec{m}_{1,N}\times\vec{H}_{1,N}^{\mathrm{eff}}\right]\\ &-\frac{\gamma\alpha_{1,N}}{(1+\alpha_{1,N}^2)}\left[\vec{m}_{1,N}\times\left[\vec{m}_{1,N}\times\vec{H}_{1,N}^{\mathrm{eff}}\right]\right]\\ &-\frac{\gamma}{M_{\mathrm{S}}a^3}\left[\vec{m}_{1,N}\times\left[\vec{m}_{1,N}\times\vec{I}_{\mathrm{L,R}}^{\mathrm{in}}\right]\right]\\ &-\frac{\gamma}{M_{\mathrm{S}}a^3}\beta\left[\vec{m}_{1,N}\times\vec{I}_{\mathrm{L,R}}^{\mathrm{in}}\right],\end{aligned} \quad (22)$$

for the magnetic moments in direct contact with the metallic parts. The last two terms in Eq. (22) stand for the spin currents $\vec{I}_{\mathrm{L,R}}^{\mathrm{in}}$ injected from the metals to the ferromagnetic chain. One of them is the torque of Slonczewski's type and the second one corresponds to an additional torque term[15,21,27]. The coefficient $\beta = 0.001$

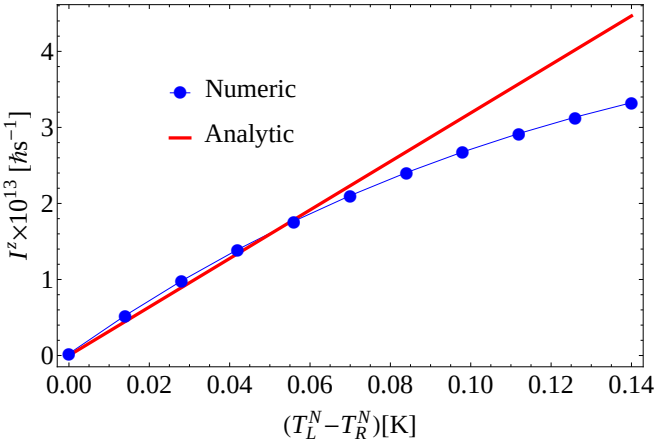

FIG. 9: Spin current through a FM cell as a function of the temperature difference of the two attached metals on the left(L) and right(R). The red curve is in line with analytical result Eq. (18), $\alpha' = 0.05$ and $T^m = 1[K]$. The blue curve corresponds to the numerical result based on Eqs. (20),(21) and (22). In the FM insulator spin torque is injected from the both left and right metals. Spin torque injected from the left metal is fixed $\lambda T_{\rm L}^N = 5\times10^{15}[\hbar s^{-1}]$ while spin torque injected from the right metal is swaped. Here $\lambda = 7.1\times10^{15}[\hbar s^{-1}T^{-1}]$ is a phenomenological constant which connects temperatures of the metals and corresponding spin torques $|\vec{I}^{\rm in}_{\rm L,R}| = \lambda T^N_{L,R}$. The spin-mixing coefficient at both interfaces (left and right) is $g_{eff} = 1.14\times10^{22}[m^{-2}]$. The temperature of the FM system is $T_F = 1[K]$. The other parameters are presented in Table I.

TABLE I: The parameters used for the $N|F|N$ system in numerical simulations

DESCRIPTION	VALUE
Anisotropy constant k, [J/m^3]	4.8×10^4
Exchange stiffness A, [J/m]	1.05×10^{-11}
Saturation magnetization $M_{\rm S}$, [A/m]	1.7×10^6
Gilbert damping α	0.01
FM cell size a, [m]	20×10^{-9}
External field H_0, [T]	10^{-5}
Number of realizations, R	100

describes the relative strength of the last torque term with respect to the Slonczewski's torque.

The results of numerical calculations are shown in the Fig. 9. We plotted the spin current conducted through the FM insulator. In numerical calculations, the FM insulator is modeled by a chain of coupled magnetic moments. The spin current is plotted as a function of temperature difference between two metals $T_L^N - T_R^N$. As we see numerical result fits the analytical behavior (Eq. (18)). Until the difference between metal temperatures is not too large, the spin current increases linearly with the difference $T_L^N - T_R^N$.

VII. CONCLUSIONS

We have studied the influence of in-plane magnetic anisotropy on the thermally activated spin current flowing through interfaces between ferromagnetic insulator and nonmagnetic metal. We have considered two different systems: (i) ferromagnetic insulator and nonmagnetic metal in a direct contact, $N|F$, and (ii) ferromagnetic insulator sandwiched between two nonmagnetic metals, $N|F|N$ structure. In the symmetric case, $K_x = K_y$, we derived analytical expressions for the average spin current in several limiting situations.

In the case of a weak anisotropy and a weak external field, $M_sVH_0/k_BT_F^m < 1$ and $H_AM_sV/2k_BT_F^m < 1$ (this case refers to the high magnon temperature T_F^m), the total spin current is given by the formula $\langle I_{sz}\rangle = 2\alpha' k_B \frac{M_sVH_0}{3k_BT_F^m}\left(T_F^m - T_N\right)\left(1 - \frac{2}{3}\frac{H_AM_sV}{2k_BT_F^m}\right)$. The in-plane positive anisotropy, $H_A > 0$, suppresses then the spin current, while the negative anisotropy, $H_A < 0$, enhances the spin current.

In the case of a strong magnetic field and a weak anisotropy, $\frac{1}{2}H_AM_sV << k_BT_F^m << H_0M_sV$, we identified a different regime, and the expression for the spin current reads then $\langle I_{sz}\rangle = 2\alpha' k_B\left(T_F^m - T_N\right)\left(1 - \frac{3H_A}{H_0}\frac{k_BT_F^m}{M_sVH_0}\right)$. In this case, the magnetic anisotropy suppresses the spin current, too. The situation is different in the asymmetric case of $K_x \neq K_y$. We find that for a weak magnetic field, $2H_0/\left(K_x + K_y\right) < 1$, the asymmetry reduces the spin current, see Fig. 4.

Another conclusion is that if the difference between temperatures T_{N1} and T_{N2} of the two metals in the $N|F|N$ system is not too large, the problem becomes effectively symmetric. The spin pumping currents flowing in opposite directions compensate then each other, $\vec{I}_{sp1} = -\vec{I}_{sp2}$, so that only the spin-torque components contribute to the total spin current. In this case, the ferromagnetic element of the structure serves as a conductor, which conducts the spin-torque current from the hot to cold metal. In the linear response regime, the spin current is linear in the temperature difference $(T_{N1} - T_{N2})$. If the difference between the temperatures of two metals is large enough, this breaks the symmetry between the spin pumping currents, $\vec{I}_{sp1} \neq -\vec{I}_{sp2}$ driving the system beyond the linear response regime.

Acknowledgements

This work has been partly supported by the National Science Center in Poland by the Grant DEC-2012/04/A/ST3/00372 (VKD and JB) and the DFG through SFB762.

Appendix A: Average values of the magnetization components

The mean components of the magnetization, see Eq. (7), are given as

$$\langle m_z\rangle = \frac{2\pi}{Z}e^B \int\limits_{-1}^{+1} dx\, x e^{Ax-Bx^2} I_0(\zeta), \tag{A1}$$

$$\langle 1-m_z^2\rangle = \frac{2\pi}{Z}e^B \int\limits_{-1}^{+1} dx\, \left(1-x^2\right) e^{Ax-Bx^2} I_0(\zeta), \tag{A2}$$

$$\langle m_z m_x^2\rangle = \frac{\pi}{Z}e^B \int\limits_{-1}^{+1} dx\, x\left(1-x^2\right) e^{Ax-Bx^2} [I_0(\zeta)+I_1(\zeta)], \tag{A3}$$

$$\langle m_z m_y^2\rangle = \frac{\pi}{Z}e^B \int\limits_{-1}^{+1} dx\, x\left(1-x^2\right) e^{Ax-Bx^2} [I_0(\zeta)-I_1(\zeta)], \tag{A4}$$

where

$$Z = 2\pi e^B \int\limits_{-1}^{+1} dx\, e^{Ax-Bx^2} I_0(\zeta) \tag{A5}$$

and $\zeta = \Delta\left(1-x^2\right)$, while $I_0(\cdots)$ and $I_1(\cdots)$ are the modified Bessel functions of the zeroth and first order, respectively. Apart from this, we introduced here the following notation: $B = \frac{1}{2}(B_x+B_y)$ and $\Delta = \frac{1}{2}(B_x-B_y)$.

In case of a weak magnetic anisotropy, $B_x = B_y = B < 1$, the spin current and the mean components of the magnetization take the form

$$\begin{aligned}\langle I_{sz}\rangle &= 2\alpha' k_B\left(T_F^m - T_N\right)\\ &\times\left\{L(A) - 2B\Big(\frac{3L(A)}{A^2}+\frac{L^2(A)}{A}-\frac{1}{A}\Big)\right\}\end{aligned} \tag{A6}$$

$$\langle m_z\rangle = L(A) - 2B\Big(\frac{3L(A)}{A^2}+\frac{L^2(A)}{A}-\frac{1}{A}\Big), \tag{A7}$$

$$\langle 1-m_z^2\rangle = \frac{2L(A)}{A} - 4B\Big(\frac{6L(A)}{A^3}+\frac{L^2(A)}{A^2}-\frac{2}{A^2}\Big), \tag{A8}$$

$$\begin{aligned}\langle m_z(m_x^2+m_y^2)\rangle &= -\frac{6L(A)}{A^2}+\frac{2}{A}\\ &+4B\Big(\frac{30L(A)}{A^4}+\frac{L(A)}{A^2}+\frac{3L^2(A)}{A^3}-\frac{10}{A^3}\Big),\end{aligned} \tag{A9}$$

where $L(A) = \coth(A) - \frac{1}{A}$ is the Langevin function.

[1] K. Uchida, S. Takahashi, K. Harii, J. Ieda, W. Koshibae, K. Ando, S. Maekawa, and E. Saitoh, Nature **455**, 778 (2008).

[2] M. Hatami, G. E. W. Bauer, Q. Zhang, and P. J. Kelly, Phys. Rev. B **79**, 174426 (2009); A. D. Avery, M. R. Pufall, and B. L. Zink, Phys. Rev. Lett.**109**, 196602 (2012); C. H. Wong, H. T. C. Stoof, and R. A. Duine, Phys. Rev. A **85**, 063613 (2012); N. Roschewsky, M. Schreier, A. Kamra, F. Schade, K. Ganzhorn, S. Meyer, H. Huebl, S. Geprägs, R. Gross, Sebastian T. B. Goennenwein Appl. Phys. Lett. **104**, 202410 (2014); D. Qu, S.Y. Huang, Jun Hu, Ruqian Wu, and C. L. Chien Phys.Rev.Lett. **110**, 067206 (2013).

[3] S. Bosu, Y. Sakuraba, K. Uchida, K. Saito, T. Ota, E. Saitoh, and K.Takanashi, Phys. Rev. B **83**, 224401 (2011); C. M. Jaworski, R. C. Myers, E. Johnston-Halperin, J. P. Heremans, Nature **487**, 210 (2012); D. G. Rothe, E. M. Hankiewicz, B. Trauzettel, and M. Guigou, Phys. Rev. B **86**, 165434 (2012); K.S. Tikhonov, J. Sinova, A.M. Finkel'stein, Nature Commun., **4**, 145 (2013).

[4] C. M. Jaworski, J. Yang, S. Mack, D. D. Awschalom, J. P. Heremans and R. C. Myers, Nat. Mater. **9**, 898 (2010); A. Slachter, F. L. Bakker, and B. J. van Wees, Phys. Rev. B **84**, 020412(R) (2011); F. K. Dejene, J. Flipse, and B. J. van Wees, Phys. Rev. B **86**, 024436 (2012); N. Li, J. Ren, L. Wang, G. Zhang, P. Hänggi, B. Li, Rev.Mod. Phys. **84**, 1045 (2012); R.F.Evans, D.Hinzke, U.Atxitia, R.W.Chantrell and O.Chubykalo-Fesenko Phys. Rev. B **85**, 014433 (2012); K.M.Lebecki, D.Hinzke, U.Nowak and O.Chubykalo-Fesenko Phys. Rev.B **86**, 094409 (2012)

[5] K. Uchida, J. Xiao, H. Adachi, J. Ohe, S. Takahashi, J. Ieda, T. Ota, Y. Kajiwara, H. Umezawa, H. Kawai, G. Bauer, S. Maekawa, and E. Saitoh, Nat. Mater. **9**, 894 (2010); S. M. Rezende, R. L. Rodriguez-Suarez, J. C. Lopez Ortiz, and A. Azevedo Phys. Rev. B **89**, 134406 (2014); S. M. Rezende, R. L. Rodriguez-Suarez, R. O. Cunha, A. R. Rodrigues, F. L. A. Machado, G. A. Fonseca Guerra, J. C. Lopez Ortiz, and A. Azevedo Phys. Rev. B **89**, 014416 (2014)

[6] J. Xiao, G. E. W. Bauer, K. Uchida, E. Saitoh, and S. Maekawa, Phys. Rev. B **81**, 214418 (2010).

[7] K. Uchida, T. Nonaka, T. Ota, H. Nakayama, and E. Saitoh, Appl. Phys. Lett. **97**, 262504(2010); D. Qu, S.Y. Huang, J. Hu, R. Wu, and C. L. Chie, Phys. Rev. Lett. **110**, 067206 (2013); M. Weiler, H. Huebl, F. S. Goerg, F. D. Czeschka, R. Gross, and S. T. B. Goennenwein, Phys. Rev. Lett.**108**, 176601 (2012); M. R. Sears and W. M. Saslow, Phys. Rev. B **85**, 035446 (2012).

[8] M. R. Sears and W. M.Saslow Phys. Rev. B **85**, 035446 (2012); R. Jansen, A. M. Deac, H. Saito, and S. Yuasa, Phys. Rev. B **85**, 094401 (2012); J.-E. Wegrowe and H.-J. Drouhin D. Lacour Phys. Rev. B **89**, 094409 (2014)

[9] J. Torrejon, G. Malinowski, M. Pelloux, R. Weil, A. Thiaville, J. Curiale, D. Lacour, F. Montaigne, and M. Hehn, Phys. Rev. Lett. **109**, 106601 (2012).

[10] N. Li, J. Ren, L. Wang, G. Zhang, P. Hänggi, B. Li, Rev. Mod. Phys. **84**, 1045 (2012); J. Ren, Phys. Rev. B **88**,220406(R) (2013); J. Borge, C. Gorini, and R. Raimondi, Phys. Rev. B **87**, 085309 (2013); S.Y. Huang, X. Fan, D. Qu, Y. P. Chen, W. G. Wang, J. Wu, T.Y. Chen, J.Q. Xiao, and C. L. Chien, Phys. Rev. Lett. **109**, 107204(2012).

[11] C.-L. Jia and J. Berakdar, Phys. Rev. B **83**, 180401R(2011).

[12] H. Adachi, K. Uchida, E. Saitoh, and S. Maekawa, Rep. Prog. Phys. **76**, 036501 (2013).

[13] Y. Tserkovnyak, A. Brataas, and G. E. W. Bauer, Phys. Rev. Lett. **88**, 117601 (2002).

[14] L. Chotorlishvili, Z. Toklikishvili, V. K. Dugaev, J. Barnaś, S. Trimper, and J. Berakdar Phys. Rev. B **88**, 144429 (2013).

[15] S. R. Etesami, L. Chotorlishvili, A. Sukhov, and J. Berakdar, Phys. Rev. B **90**, 014410 (2014).

[16] S. Hoffman, K. Sato, and Y. Tserkovnyak, Phys. Rev. B **88**, 064408 (2013).

[17] M. Agrawal, V. I. Vasyuchka, A. A. Serga, A. D. Karenowska, G. A. Melkov, and B. Hillebrands, Phys. Rev.Lett. **111**, 107204 (2013).

[18] T. Kikkawa, K. Uchida, S. Daimon, Y. Shiomi, H. Adachi, Z. Qiu, D. Hou, X.-F. Jin, S. Maekawa, and E. Saitoh Phys. Rev. B **88**, 214403 (2013); M. Schreier, A. Kamra,M. Weiler, J. Xiao, G. E. W. Bauer, R. Gross, and S. T. B. Goennenwein, Phys. Rev. B **88**, 094410 (2013).

[19] W. F. Brawn Phys. Rev. **130**, 1677 (1963); W. T. Coffey and Y. P. Kalmykov J. Appl. Phys. **112**, 121301 (2012).

[20] T. Bose and S. Trimper Phys. Rev. B **81**, 104413 (2010); U.Atxitia, O.Chubykalo-Fesenko Phys. Rev. B **84** 144414 (2011).

[21] A. Kapelrud and A. Brataas, Phys. Rev. Lett. **111**, 097602 (2013).

[22] M. Schmid, S. Srichandan, D. Meier, T. Kuschel, J.-M. Schmalhorst, M. Vogel, G. Reiss, C. Strunk, and C. H. Back Phys. Rev. Lett. **111**, 187201 (2013)

[23] P. E. Kloeden, *Numerical Solution of SDE Through Computer Experiments* (Springer Science, Business Media, Berlin, 1994).

[24] A. Sukhov, J. Berakdar, Phys. Rev. B **79**, 134433 (2009); Phys. Rev. Lett **102**, 057204 (2009).

[25] L. Chotorlishvili, Z. Toklikishvili, A. Sukhov, P. P. Horley, V. K. Dugaev, V. R. Vieira, S. Trimper, and J. Berakdar, J. Appl. Phys. **114**, 123906 (2013).

[26] X. Joyeux, T. Devolder, Joo-Von Kim, Y. Gomez de la Torre, S. Eimer, and C. Chappert J. of Appl. Phys. **110**, 063915 (2011).

[27] A. Brataas, A. D. Kent, and H.Ohno, Nat. Mater. 11, 372 (2012).